Quasicontinuous decay and properties of superdeformed excitations in ^{195}Pb

M. S. Johnson,[1,*] J. A. Cizewski,[1] K. Y. Ding,[1,†] N. Fotiades,[1,‡] M. B. Smith,[1,§] J. S. Thomas,[1] W. Younes,[1,‖] J. A. Becker,[2]
L. A. Bernstein,[2] K. Hauschild,[2,¶] D. P. McNabb,[2] M. A. Deleplanque,[3] R. M. Diamond,[3] P. Fallon,[3] I. Y. Lee,[3]
A. O. Macchiavelli,[3] and F. S. Stephens[3]

[1]*Department of Physics and Astronomy, Rutgers University, New Brunswick, New Jersey 08903*
[2]*Lawrence Livermore National Laboratory, Livermore, California 94550*
[3]*Lawrence Berkeley National Laboratory, Berkeley, California 94720*
(Received 18 October 2004; published 21 April 2005)

Superdeformed excitations in ^{195}Pb were populated via the ^{174}Yb(^{26}Mg,5n) reaction, and γ-ray spectroscopy measurements were made with Gammasphere. Analysis of the intensities of the discrete transitions between superdeformed states indicates that the decay out occurs from the favored band of the lowest signature pair. The quasicontinuous spectra associated with the decay of superdeformed bands in ^{195}Pb have been extracted for both signatures. The onset of γ-ray intensity and the normalized γ-ray intensity of the quasicontinuum decay spectrum are used to set a lower bound of 2.5 MeV at $\sim$11$\hbar$ for superdeformed excitation energy relative to normal deformed excitations in ^{195}Pb.

I. INTRODUCTION

The evidence for metastable superdeformed (SD) excitations has been one of the most intriguing discoveries of modern nuclear physics. The accepted model illustrated in Fig. 1(a) for describing such nuclei is one in which a secondary minimum exists at large prolate deformations with an inner barrier of depth W_I and an outer barrier determined by the fission barrier with height E_s. The attenuation of the lower-lying SD band transitions suggests [1] that the states in the SD well mix with excitations with similar energies and quantum numbers in the adjacent normal deformed (ND) well. The transition matrix elements favor the higher γ-ray energies to low-lying ND states. The study of the decay of SD excitations can be used to determine excitation energies and spins of SD states. The best method to determine energies and spins of SD states is to measure the direct transition that links one SD state to a low-lying ND state. By using the known excitation energy and spin of the final ND state, the energy, spin, and parity of the SD state can be deduced. However, these single-step γ-ray transitions are a small part of the SD decay spectrum and are further suppressed for SD states with high excitation energy. Rather, the majority of the decay occurs via multistep pathways which cannot be resolved, forming a quasicontinuous (QC) decay spectrum. However, by extracting the QC decay spectrum and normalizing the decay intensity to one cascade, the average spin and average energy lost in

a typical decay can be measured and an estimate of spin and energy of SD excitations deduced.

The quasicontinuous decay spectrum from SD structures in $A \sim 190$ nuclei can also be used to probe level densities and γ-ray strength functions that characterize ND excitations at finite temperature and spin where pairing effects are present. Since the decay of SD excitations is understood [1] to occur because of mixing with ND excitations at similar spins and excitation energies, the shape of the SD decay spectrum is that of the ND excitations with which the SD states mixed. For $A \sim 190$ nuclei, the shape of the QC decay spectrum is expected to depend on pairing effects in the ND well at low spin ($\sim$10$\hbar$). This is in contrast to $A \sim 150$ SD nuclei, which decay out at much higher spins where ND pairing effects are quenched. Pairing has the largest effect on the QC decay spectrum in even-even nuclei where the like nucleons are paired, giving rise to a gap G in the ND level density between the yrast state and the next excited state for a given spin. For odd-even and odd-odd nuclei, no gap in the ND level density is expected; therefore, the shape of the decay spectrum should be noticeably different, with a smooth increase in γ-ray intensity as γ-ray energy decreases.

The present work studies the QC decay of SD excitations in the odd-mass ^{195}Pb. Superdeformed states in ^{195}Pb were first observed by Farris and coworkers [2], who assigned the lowest two bands as signature partner pairs of the 7_3 neutron intruder orbital, $5/2^-$ [752]. The spin values were assigned from comparison of the lowest observed transition in each band to a rigid rotor. Further work on SD ^{195}Pb by Severen et al. [3] supported the orbital assignment by Farris et al. and extracted the quadrupole moment from lifetime measurements. In Gammasphere Phase I, Hauschild and collaborators [4] conducted an experiment to search for direct one-step transitions between SD states and low-lying ND states in ^{195}Pb to determine excitation energies, spins, and parities of SD excitations. The search was unsuccessful; however, that dataset has been used in the present work to investigate the QC decay of SD excitations in ^{195}Pb.

*Present address: Oak Ridge Associated Universities, Oak Ridge, TN 37831.
†Present address: Telecordia Technology, Piscataway, NJ 08854.
‡Present address: Los Alamos National Laboratory, Los Alamos, NM 87545.
§Present address: Bubble Technology Industries, P.O. Box 100, Highway 17, Chalk River, Ontario, Canada K0J 1J0.
‖Present address: Lawrence Livermore National Laboratory, Livermore, CA 94550.
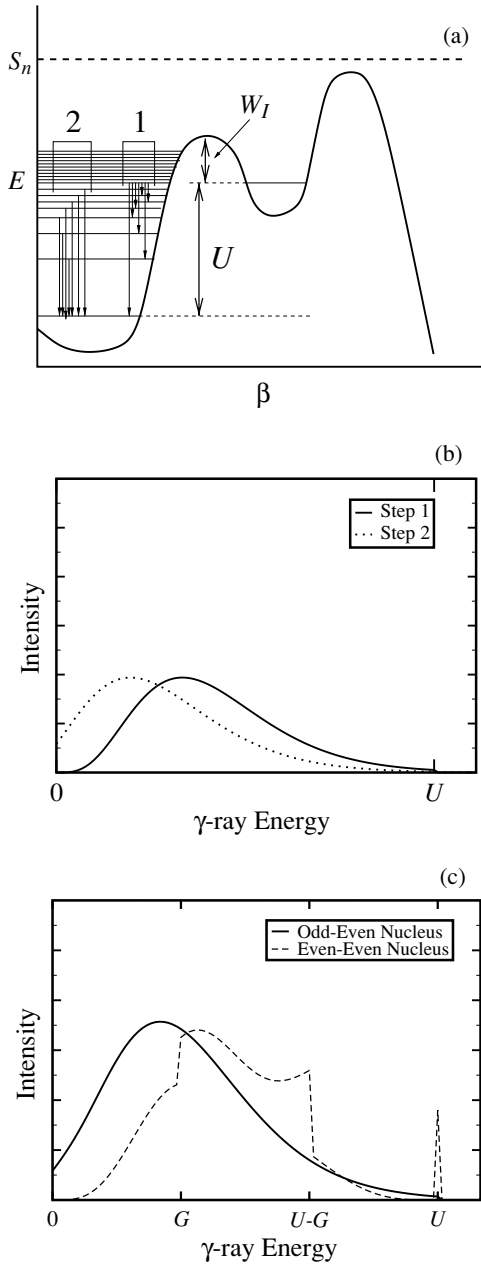¶Present address: CSNSM, Orsay Cedex F-91405, France.

FIG. 1. (a) Schematic model of two-step SD decay. (b) Simulated γ-ray spectra (two steps) associated with the decay of a SD state when there is no gap in the ND level density. (c) Comparison of decay spectra for decay with no gap in ND level density (solid curve) versus decay with a gap G in ND level density (dashed curve). (See text for more details.)

II. EXPERIMENTAL SETUP

High-spin states of ^{195}Pb were populated using the ^{174}Yb(^{26}Mg,5n) reaction with a beam energy of 132 MeV. The measurements were made using the Gammasphere Phase I array at the 88-Inch Cyclotron Facility at the Lawrence Berkeley National Laboratory. The array was composed of 95 Ge detectors with the Hevimet collimators in place. Two ^{174}Yb targets of thickness 1.03 mg/cm^2 and 960 μg/cm^2

evaporated onto $\sim$8-mg/cm^2 gold backings were used. A total of 1.1×10^9 threefold events were collected for analysis.

III. MODEL OF QUASICONTINUOUS DECAY OF SUPERDEFORMED EXCITATIONS

A simple model has been developed to describe some important features expected for the SD decay spectrum for the odd-mass nucleus ^{195}Pb. It is assumed [1] that the decay of SD excitations occurs via mixing with ND excitations at similar excitation energy and spin. The SD decay spectrum, therefore, reflects the decay of the ND state. Assuming that the γ-ray transitions associated with the decay of the ND state are dominated by $E1$ transitions, the γ-ray intensity for each step is

$$I_\gamma \sim E_\gamma^4 \rho(E_f), \tag{1}$$

where the $E1$ strength function E_γ^4 is consistent with the parametrization chosen by Døssing *et al.* [5] to reflect the tail of the giant dipole resonance for $E1$ transitions. The level density $\rho(E_f)$ is assumed to be the constant temperature parametrization:

$$\rho(E_f) = e^{E_f/T}, \tag{2}$$

where T is the temperature and $E_f = U - E_\gamma$, where U is the energy above yrast. Pairing effects are neglected to simplify the model but are addressed in more realistic calculations [5].

The general picture for decay from a SD state is illustrated in Fig. 1. A two-step process is considered, where the first steps are transitions from the excited level U to levels above the yrast state. The second steps are transitions from levels populated in the first step to the yrast state. Normalizing the intensity to the initial level density, the γ-ray intensity associated with the first step becomes

$$I_\gamma \sim E_\gamma^4 e^{-E_\gamma/T}, \tag{3}$$

as illustrated in Fig. 1(b). The available phase space open to the first step is from $E_\gamma = 0$ to $E_\gamma = U$. The second step is similar, but the centroid is shifted to lower E_γ because of the low probability that the highest energy states were populated in step 1. Again the range extends from $E_\gamma = 0$ to $E_\gamma = U$. Adding these two spectra yields the total spectrum in Fig. 1(c) (solid curve) that one would expect for decay of an SD state with no gap in the ND level density. Adding a third step would produce a spectrum similar to step 1 but again shifted to lower E_γ as in step 2. Extra steps are neglected here to maintain the simplicity of the model. For comparison, the QC decay-out intensity for an even-even model is shown in Fig. 1(c) as the dashed curve. The even-even model is taken from [6] and normalized here to two steps.

The conclusions from this model are threefold:

- In odd-A nuclei there is a gradual increase in γ-ray intensity as γ-ray energy decreases below $E_\gamma = U$. This is in contrast to model predictions [5,6] for even-even nuclei in which a gap G in the level density causes a rapid increase in γ-ray intensity for $E_\gamma < U - G$, shown in Fig. 1(c) (dashed curve).

- The present model shows that there is a significant amount of γ-ray intensity at low energies in odd-mass nuclei. This is in contrast to the predictions for even-even nuclei where it was shown [5,6] and illustrated in Fig. 1(c) that for γ-ray energies less than the gap energy G, a small fraction of SD decay γ-ray intensity is expected.
- The decay intensity is spread out over a larger region of γ-ray energies for odd-even nuclei compared to even-even nuclei. For even-even nuclei, it was shown [7] that most of the intensity is between $E_\gamma = G$ and $E_\gamma = U - G$, as illustrated in Fig. 1(c). The comparison in Fig. 1(c) shows that the range of energies for which there is sizable γ-ray intensity associated with SD decay is U for odd-even nuclei, but $U - 2G$ for even-even nuclei. Therefore, for an equal number of steps, the even-even decay spectrum will be more pronounced above background.

The benefit of a large gap ($G \gtrsim 1$ MeV) in the level density, or higher SD excitation energy, is that the QC decay spectrum can be cleanly separated from the quasicontinuous feeding structures, which dominate at energies typically less than 1 MeV. For nuclei with a small gap or no gap in the level density, or low SD excitation energies, the analysis is considerably more complicated.

IV. DISCRETE γ-RAY TRANSITIONS ASSOCIATED WITH SD ^{195}Pb

The total γ-ray spectra gated on known [2] SD transitions for bands 1 and 2 in ^{195}Pb were extracted and are displayed in Fig 2. The partial level scheme associated with SD bands 1 and 2 in ^{195}Pb is displayed in Fig. 3, illustrating the lower excitation parts of both bands, as well as the placement of ND transitions observed in coincidence with these SD bands. The original band assignments were made by Farris and coworkers [2], where it was determined that the crosstalk between bands 1 and 2 was evidence that the bands are signature pairs of the 7_3 $5/2^-[752]$ neutron intruder orbital, an assignment confirmed by Severen *et al.* [3]. However, the relative placement of the bands was not clear. By analyzing the spectrum in coincidence with the 203-keV transition of band 2, it was noted that the 182- and 222-keV transitions were not present. This and similar coincidence relations support the relative placement in Fig. 3. The transition intensities are listed in Table I. Transitions used in the gating are noted and are identical to the gates used in [2].

The depopulation of band 2 to ND states starts at the level fed by the 244-keV transition. This has been verified by observing gates above, below, and including the 244-keV transition. The 618-keV transition is in coincidence with SD transitions of 244 keV and higher, and it was previously assigned as depopulating the $25/2^+$ ND level [8]. Therefore, possible spin-parity assignments for the level fed by the 244-keV transition are $25/2^\pm$, $27/2^\pm$, and $29/2^+$, assuming $\Delta J \geqslant 0$ transitions of dipole or $E2$ character. Farris *et al.* [2] estimated the spin of the level fed by the 244-keV transition to be $21/2^-$. However, the uncertainty in this estimate is at least $1\hbar$, because the estimate was based solely on the lowest
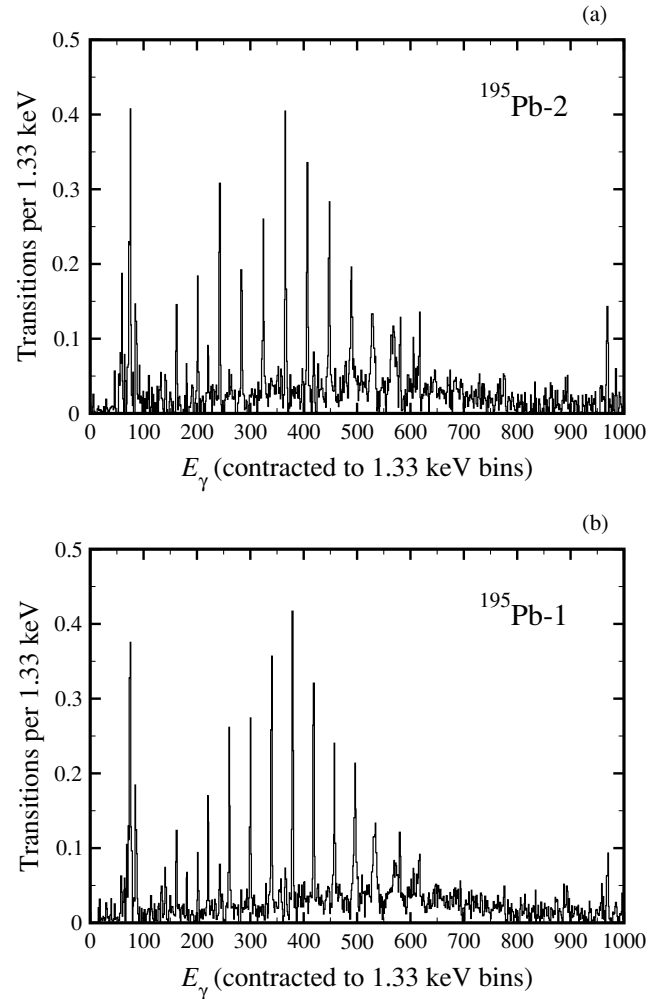

FIG. 2. Spectra gated on SD band 2 (a) and band 1 (b) in ^{195}Pb after removal of summed events, neutron-induced γ rays, and Compton-scattered photons. The spectra have been efficiency-corrected and normalized to one cascade. See text for additional details.

transition in each band. The spin-fit method [9] has been shown [10] to be sensitive to the number of data points in the fit and can vary by as much as a full unit of spin. Given the 7_3 negative-parity orbital assignment and the spin of $21/2^- \pm 1$ from the estimate by Farris *et al.* [2], $J^\pi = 25/2^-$ has been assigned to the level fed by the 244-keV SD-2 transition. The other spin-parity assignments follow from the stretched $E2$ character of intraband and assumed mixed $M1/E2$ interband SD transitions. The difference between the new and old spin assignments [2] is $2\hbar$. The present assignments preserve the comparison of the experimental and calculated routhians reported by Farris *et al.*, i.e., band 2 is the favored signature.

The results for the analysis of the discrete transitions of SD bands 1 and 2 are given in Table I. The angular distributions were extracted by fitting the spectra in each ring of Gammasphere to

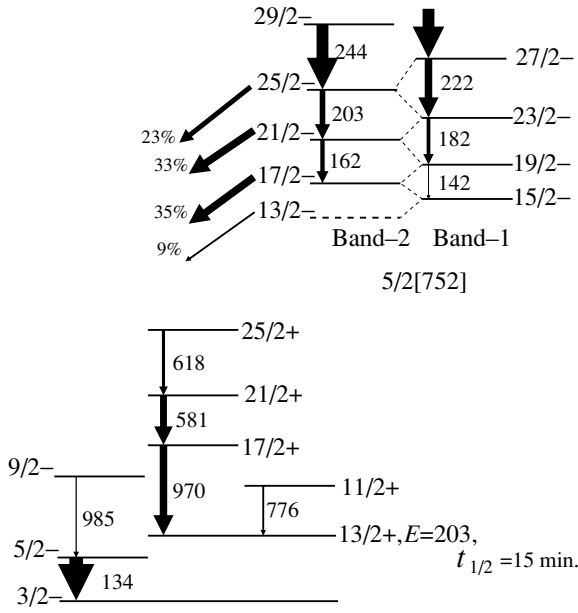$$W(\theta) = A_0 + A_2 P_2(\cos\theta). \tag{4}$$

FIG. 3. Partial level scheme of ^{195}Pb highlighting the decay region of SD bands 1 and 2 and the feeding of low-lying ND levels. The energies of the transitions are in keV. The widths of the arrows are proportional to the intensities of the observed transitions, including electron conversion. The vertical scale does not reflect relative energies.

Higher order terms are neglected in Eq. (4) due to insufficient statistics. The relative intensities were extracted from the A_0 spectra and were corrected for electron conversion as well as gating effects. The intensity profile for each band matches the profile given in [2] for those bands. The intensity profiles plateau at midband and are indicative of no side feeding, important in the analysis of the SD decay out. The intensities of known ND transitions in coincidence with either band are also given.

An interesting feature from the intensities in Table I is that for both SD bands, the intensities of the ND transitions fed by the SD decay are equal within uncertainties. This suggests a similar decay pattern for both bands. To determine how each SD band decays, the attenuated intensities of the transitions in the region of the decay were extracted. Usually, to determine exactly how SD bands decay, measuring the attenuation of intensity of the SD-band transitions is sufficient. However, for ^{195}Pb, the intensities include fluctuations associated with the interband transitions and therefore do not provide a clear measure of the decay pattern. Furthermore, these transitions between the SD bands are not observed. They are assumed to be of $M1$ character, less than 100 keV in energy and, therefore, completely electron converted. To deduce the decay pattern, we used the expression

$$\mathcal{D}_I + \mathcal{D}_{I-1} = 1 - (\mathcal{I}_{I-2} + \mathcal{I}_{I-3})|_{g:I+2 \to I}, \quad (5)$$

which states that the sum of the decay $\mathcal{D}$ out of levels with spin I and $I-1$ is equal to the difference of the band intensity, defined as unity, and the resultant intensities $\mathcal{I}$ of the transitions that depopulate levels I and $I-1$, gated on the transition

TABLE I. SD and prominent ND transitions [8] in coincidence with SD band 2 (top) and band 1 (bottom) in ^{195}Pb.

Transition (keV)	Placement	Relative intensity	$\frac{A_2}{A_0}$
Band 2			
162.20(15)[a]	$\frac{21}{2}^- \to \frac{17}{2}^-$	0.44(4)	
202.44(14)[a]	$\frac{25}{2}^- \to \frac{21}{2}^-$	0.52(5)	
243.49(3)[a]	$\frac{29}{2}^- \to \frac{25}{2}^-$	0.90(6)	0.4(1)
284.73(3)[a]	$\frac{33}{2}^- \to \frac{29}{2}^-$	≡1.00(5)	0.4(3)
325.51(4)[a]	$\frac{37}{2}^- \to \frac{33}{2}^-$	0.95(6)	0.4(2)
366.57(3)[a]	$\frac{41}{2}^- \to \frac{37}{2}^-$	0.99(6)	0.3(1)
407.79(11)[a]	$\frac{45}{2}^- \to \frac{41}{2}^-$	0.99(6)	0.3(1)
448.76(14)[a]	$\frac{49}{2}^- \to \frac{45}{2}^-$	0.99(6)	0.4(2)
489.09(19)[a]	$\frac{53}{2}^- \to \frac{49}{2}^-$	0.87(6)	
530.44(28)	$\frac{57}{2}^- \to \frac{53}{2}^-$	0.67(7)	
569.87(39)	$\frac{61}{2}^- \to \frac{57}{2}^-$	0.57(7)	
970(ND)	$\frac{17}{2}^+ \to \frac{13}{2}^+$	0.35(4)	
581(ND)	$\frac{21}{2}^+ \to \frac{17}{2}^+$	0.30(4)	
618(ND)	$\frac{25}{2}^+ \to \frac{21}{2}^+$	0.17(4)	
776(ND)	$\frac{11}{2}^+ \to \frac{13}{2}^+$	0.12(4)	
985(ND)	$\frac{9}{2}^- \to \frac{5}{2}^-$	0.13(3)	
134(ND)	$\frac{5}{2}^- \to \frac{3}{2}^-$	0.53(3)	
Band 1			
141.8(2)	$\frac{15}{2}^- \to \frac{11}{2}^-$	0.09(2)	New[b]
181.94(18)[a]	$\frac{23}{2}^- \to \frac{19}{2}^-$	0.35(2)	
222.03(14)[a]	$\frac{27}{2}^- \to \frac{23}{2}^-$	0.63(3)	
261.96(10)[a]	$\frac{31}{2}^- \to \frac{27}{2}^-$	0.87(3)	0.4(2)
301.33(10)[a]	$\frac{35}{2}^- \to \frac{31}{2}^-$	0.99(3)	0.4(1)
340.93(9)[a]	$\frac{39}{2}^- \to \frac{35}{2}^-$	≡1.00(4)	0.4(1)
380.51(14)[a]	$\frac{43}{2}^- \to \frac{39}{2}^-$	0.98(4)	0.5(2)
419.72(19)[a]	$\frac{47}{2}^- \to \frac{43}{2}^-$	0.94(4)	0.4(1)
458.55(22)[a]	$\frac{51}{2}^- \to \frac{47}{2}^-$	0.83(4)	
497.39(22)[a]	$\frac{55}{2}^- \to \frac{51}{2}^-$	0.65(5)	
534.6(3)	$\frac{59}{2}^- \to \frac{55}{2}^-$	0.60(4)	
574.1(8)	$\frac{63}{2}^- \to \frac{59}{2}^-$	0.38(6)	
970(ND)	$\frac{17}{2}^+ \to \frac{13}{2}^+$	0.32(2)	
581(ND)	$\frac{21}{2}^+ \to \frac{17}{2}^+$	0.30(3)	
618(ND)	$\frac{25}{2}^+ \to \frac{21}{2}^+$	0.15(2)	
776(ND)	$\frac{11}{2}^+ \to \frac{13}{2}^+$	0.10(2)	
985(ND)	$\frac{9}{2}^- \to \frac{5}{2}^-$	0.08(2)	
134(ND)	$\frac{5}{2}^- \to \frac{3}{2}^-$	0.58(2)	

[a]Gating transition.
[b]New transition assigned to SD band 1.

feeding level I. This formula was applied to each level for each band after the point at which both bands are completely fed. The result was a set of equations, each of which had two unknowns $\mathcal{D}_I$ and $\mathcal{D}_{I-1}$, which generated N equations with $N+1$ unknowns. The ability to solve this system of equations came from the gate on the 284-keV transition in which the intensities of the 244- and 222-keV transitions summed to
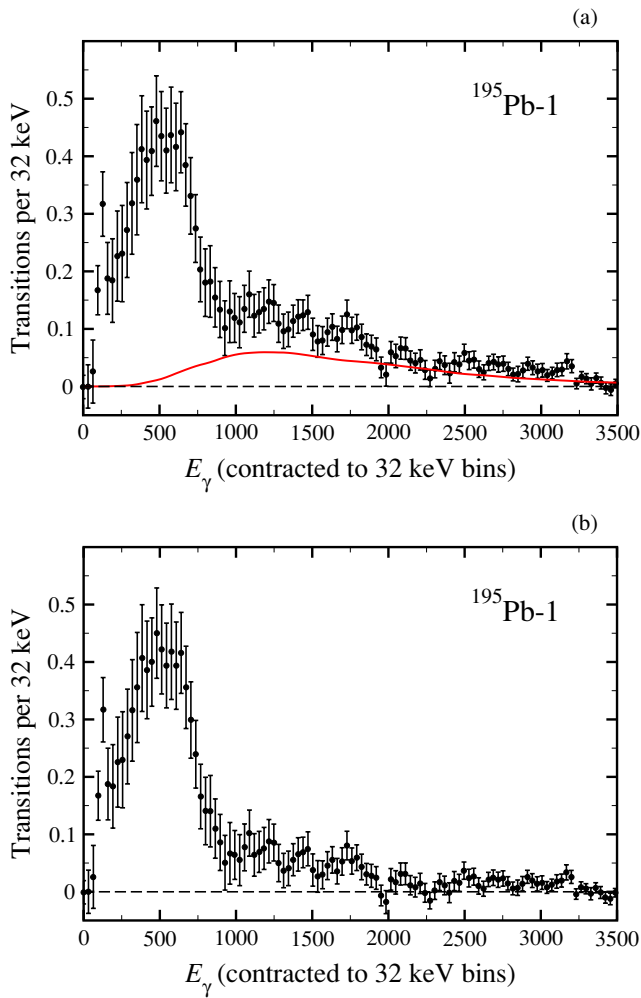
FIG. 4. (Color online) (a) Unresolved spectrum associated with SD band 1 in ^{195}Pb and model calculation for statistical mode of feeding. (b) Unresolved spectrum associated with SD band 1 in ^{195}Pb after subtraction of the statistical spectrum.

unity. This implied not only that the decays out of the $27/2^-$ and $29/2^-$ SD levels were zero, but that individually the decays from these levels were zero, since $\mathcal{D}$ is positive definite. This reduced the number of unknowns to the number of equations. The resulting decay-out pattern is summarized in Fig. 3.

V. QUASICONTINUOUS DECAY OF SD ^{195}Pb

To extract the unresolved intensity associated with SD decay, the approach first used in [11], improved by [12], and used in other Pb isotopes [6] was adopted for the analysis of SD bands 1 and 2 in ^{195}Pb. Details of this procedure are outlined in [13]. The focus of this analysis is to identify the different components of the γ-ray spectrum and remove those components to separate the SD decay component. The different components of the spectra include: statistical $E1$ decay from the evaporation-residue; unresolved feeding components of

higher excited SD bands into the SD yrast band, which includes $E2$ and admixed $M1/E2$ components; discrete SD yrast transitions; resolved and unresolved transitions associated with the decay of the SD yrast band; and known ND transitions.

The unresolved part of the γ-ray spectrum of ^{195}Pb SD band 1, after removing discrete transitions, is displayed in Fig. 4. Although this work shows that the decay occurs from levels in band 2, the decay from band 1 is the same as that from band 2 because of the strong coupling of the two bands via interband transitions. The analysis of the quasicontinuous (QC) decay of both bands confirmed that indeed the two decay spectra are identical. The QC spectrum for band 1 is preferred over that of band 2 because of enhanced statistics. In the analysis of SD band 1, the gating transitions had fewer contaminants, in contrast to SD band 2 where many of the transitions are similar in energy to those of fission fragments, Coulomb excitation, and other contaminants not associated with SD ^{195}Pb. Also shown in Fig. 4 is a spectrum of $E1$ statistical transitions obtained from calculations for ^{192}Hg [14], normalized to the intensity of the unresolved spectrum above 3 MeV. This same spectrum of statistical transitions was used in the analysis of ^{194}Pb [6], where it was assumed to be appropriate because of the similar shapes at high γ-ray energy where the intensity in this region is predominantly statistical transitions. The same argument is used in this work for ^{195}Pb, because no differences are expected between the statistical feeding of ^{195}Pb and ^{194}Pb. Furthermore, a good fit of the calculation [14] to the data for $E_\gamma \gtrsim 2$ MeV has been made with a $\chi^2_\nu = 1.190$.

After subtracting the statistical spectrum, the resultant QC spectrum with feeding and decay components is displayed in Fig. 4(b). The nonzero component between 900 keV and about 1.8 MeV is associated with the decay of SD ^{195}Pb, since it is consistent with transitions emitted in a stopped frame. However, a significant part of the γ-ray intensity associated with SD decay is expected below 1 MeV. There is no clear distinction between the SD feeding and decay components around 900 keV, apart from angular distributions displayed in Fig. 5. It is evident in Fig. 5 that the $E2$ bump, associated with $E2$ SD feeding transitions, is located at $\sim$800 keV because the A_2/A_0 values are consistent with the known $E2$ in-band
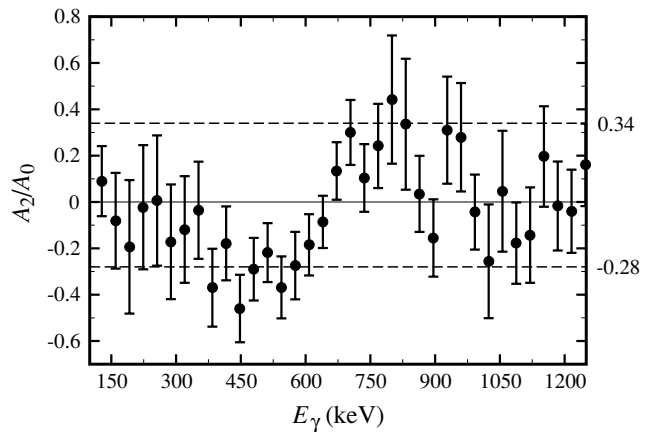

FIG. 5. Angular distribution spectrum, A_2/A_0, in the center-of-mass frame of the QC spectrum associated with SD ^{195}Pb band 1.
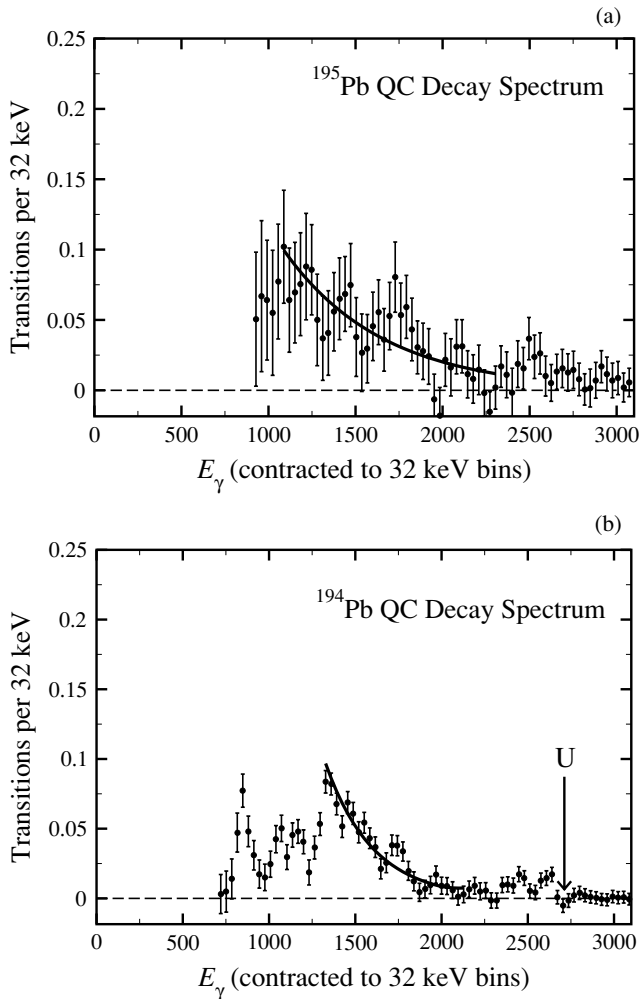
FIG. 6. (a) Unresolved spectrum associated with QC decay of SD band 1 in ^{195}Pb with an exponential fit. (b) Unresolved spectrum associated with QC decay of SD ^{194}Pb with exponential fit of high-energy tail.

transitions given in Table I. The location of the $E2$ bump at $\sim$800 keV is similar to the location of the $E2$ bump for ^{194}Pb [7]. The negative values at lower γ-ray energies are attributed to $M1/E2$ feeding. The thresholds for the angular distributions described by the dashed lines in Fig. 5 were determined by average values of angular distribution coefficients measured in Table I and those given in Ref. [15].

Further support that the nonzero component between 900 keV and 1.8 MeV is associated with SD decay and not with the current model [14] for statistical feeding comes from the fit of the data to model calculations in that region. This fit yields a $\chi_\nu^2 = 3.477$, much worse than the fit to the high E_γ region discussed above.

The QC decay spectra for ^{195}Pb (band 1) and ^{194}Pb [6] are displayed in Figs. 6(a) and 6(b), respectively. The energy above yrast, U, of the ^{194}Pb SD band has been determined from the discrete transitions [16,17] observed to connect SD and ND states. To quantify the description of these QC decay spectra, the tails of these spectra have been fit by an exponential. For both ^{195}Pb and ^{194}Pb (as well as ^{192}Pb [6]), the onset

of QC decay intensity starts at $\sim$2.2 MeV. However, the QC decay intensity in ^{195}Pb increases gradually (with slope $-0.0017(14)$) for γ-ray energies below 2.2 MeV, in contrast to ^{194}Pb where the γ-ray intensity increases more rapidly (with slope $-0.0036(4)$) below $\sim$1.8 MeV to a maximum within 500 keV. The steeper rise in intensity for ^{194}Pb compared to ^{195}Pb is expected for a nucleus with a finite gap G in the level density. With a gap in level density, the QC decay intensity is predominantly in the range of $G < E_\gamma < U - G$ and therefore more pronounced [see Ref. [6] and Fig. 1(c)] than the broader region of $0 < E_\gamma < U$ covered by nuclei with no gap in level density. Finally, the overlap of the feeding components and the QC decay spectrum in Fig. 4(b) is interpreted to mean that the QC decay intensity extends to lower energies in ^{195}Pb in contrast to ^{194}Pb [6] where a significant portion (95%) of the QC decay intensity in Fig. 6(b) is in the region $E_\gamma \geqslant 0.95$ MeV. For an odd-even nucleus, such as ^{195}Pb, a significant portion of the QC decay intensity is expected to extend to $E_\gamma = 0$ (see Fig. 1) if the model discussed above is correct.

Since the QC decay spectrum for SD ^{195}Pb cannot be separated from the feeding components, no definite values can be extracted for average energy and spin carried away by the decay. However, limits can be determined using the tail region of the decay spectrum above 900 keV, and the results are given in Table II. Since the data in Fig. 6 are normalized to one cascade, the integral of a given region will give an average γ-ray multiplicity $m_\gamma \equiv \bar{m}$. This will not be the total γ-ray multiplicity for the decay, since an unknown portion of the QC decay spectrum remains below 900 keV, but this sets a lower limit $\bar{m} \sim 2$. The uncertainty is statistical and does not include the uncertainties associated with the QC decay component below 900 keV, because the shape and intensity of the QC decay below 900 keV are unknown. The average γ-ray energy $\bar{E}_\gamma$ is the centroid of the tail region of the QC spectrum. The value of 1.2 MeV is an upper bound, since a sizeable decay intensity below 900 keV would shift the centroid to lower energies. Again, the uncertainties associated with $\bar{E}_\gamma$ do not include the decay component below 900 keV. By multiplying these two values together, $\bar{m} \times \bar{E}_\gamma$, the average energy taken away by the QC decay component is $\sim$2.5 MeV. Although this does not represent the entire QC decay spectrum, this value is similar to results for ^{194}Pb where $\bar{m} \times \bar{E}_\gamma = 2.7$ MeV from the analysis of the QC decay spectrum [6], a value consistent with the relative excitation energy U determined from discrete

TABLE II. Comparison of results of SD decay studies in $A \sim 190$ nuclei.[a]

Spectrum	$\bar{m}$	$\bar{E}_\gamma$	$\bar{m} \times \bar{E}_\gamma$	$\bar{m} \times \Delta I$	U
^{195}Pb	$\geqslant$2.1(6)	$\leqslant$1.2(1)	$\geqslant$2.5(7)	1.1(6)	na
^{194}Pb	1.93(16)	1.44(3)	2.7(2)	0.83(33)	2.74
^{194}Hg	2.1(2)	1.7(1)	4.2(2)	1.1(3)	4.0
^{192}Hg	2.2(2)	1.6(1)	3.9(2)	$\geqslant$1.1(2)	na
^{191}Hg	1.95	1.41	3.4(2)	3.0(6)	$\sim$3.14

[a]The average γ-ray multiplicity $\bar{m}$, average γ-ray energy $\bar{E}_\gamma$, energy and spin carried by the decay $\bar{m} \times \bar{E}_\gamma$ and $\bar{m} \times \Delta I$, and energy above yrast U are given for ^{195}Pb (present results), ^{194}Pb [6,16,17], ^{194}Hg [12,20], ^{192}Hg [12], and ^{191}Hg [19].

transitions which connect SD and ND excitations [16,17]. A calculation by Lopez-Martens *et al*. [18] for the QC decay of SD ^{192}Hg shows that for an odd-even nucleus, such as ^{195}Pb, half of the decay intensity will be greater than 1 MeV. The present estimate of $\bar{E}_\gamma \leqslant 1.2$ MeV is therefore likely to reflect an actual $\bar{E}_\gamma$ of $\sim$1.2 MeV.

The angular momentum carried off in the QC decay of SD ^{195}Pb can be estimated by $\bar{m} \times \Delta I$, where ΔI is the average spin carried off by a single transition. The dominant mode of decay can be assumed to be via $E1$ transitions, where each transition carries an average spin of $0.5\hbar$. Therefore, the spin carried off from the entire decay is on the order of $1\hbar$, a value consistent with the discrete analysis in Fig. 3.

VI. CONCLUSIONS

To summarize, the discrete and quasicontinuous γ-ray spectra associated with SD bands 1 and 2 of ^{195}Pb have been extracted and analyzed. The analysis of the discrete γ-ray transitions has shown that the decay occurs from the favored band 2 of the $5/2^-[752]$ orbital. The analysis of the QC decay spectrum has shown that the excitation energy of SD states above yrast is at least 2.5 MeV at $\sim$11$\hbar$, and the QC decay carries off about $1\hbar$ in angular momentum, results similar to those for ^{194}Pb [6].

The shape of the QC decay spectra has also shed light on the level density of ND excitations at finite spin. The gradual increase in intensity of the QC decay spectrum as γ-ray energy decreases is consistent with no gap in the ND level density, as expected for an odd-even nucleus. The gradual increase

in intensity of the QC decay spectrum is obvious in a recent paper for another odd-even nucleus, ^{191}Hg [19]. Also seen in the QC decay spectrum in ^{191}Hg [19] is the extension of the γ-ray intensity to low energies. Furthermore, in ^{191}Hg [19], the shape of the QC decay spectrum resembles the model for odd-even nuclei in Fig. 1. The fit for the QC decay spectrum in ^{191}Hg [19] to a model such as Fig. 1 is expected to be better than a model fit for an odd-even nucleus with lower relative excitation energy, such as ^{195}Pb, because the higher SD excitation energy facilitates separation of QC feeding and decay compounds.

One challenge in the present analysis was the overlap in energy of the lower part of the QC decay spectrum and the QC quadrupole and admixed $M1/E2$ feeding components. One solution would have been the successful identification of single-step transitions which connect SD levels to low-lying ND levels, thereby bypassing the QC decay. This is a difficult task because these transitions are expected to be only a few percent of the total decay; no single-step transitions were identified in the present or previous [4] analyses of SD ^{195}Pb. By gating on such linking transitions and SD transitions, the QC decay component of the spectrum could have been eliminated, and the feeding components would have been isolated.

[1] E. Vigezzi, R. A. Broglia, and T. Døssing, Phys. Lett. **B249**, 163 (1990).

[2] L. P. Farris *et al*., Phys. Rev. C **51**, 2288(R) (1995).

[3] U. J. van Severen *et al*., Phys. Lett. **B434**, 14 (1998).

[4] K. Hauschild *et al*., Bull. Am. Phys. Soc. **42**, 670 (1997).

[5] T. Døssing *et al*., Phys. Rev. Lett. **75**, 1276 (1995).

[6] D. P. McNabb *et al*., Phys. Rev. C **61**, 031304 (2000).

[7] D. McNabb, Ph.D. thesis, Rutgers University, 1997.

[8] M. Bhat, *Evaluated Nuclear Structure Data File* (Springer-Verlag, Berlin, Germany, 1992) (data extracted using online data service from ENSDF database, revised October, 2003).

[9] J. A. Becker *et al*., Phys. Rev. C **46**, 889 (1992).

[10] C. L. Wu, *et al*., Phys. Rev. Lett. **66**, 1377 (1991).

[11] R. G. Henry *et al*., Phys. Rev. Lett. **73**, 777 (1994).

[12] T. Lauritsen *et al*., Phys. Rev. C **62**, 044316 (2000).

[13] M. Johnson, Ph.D. thesis, Rutgers University, 2003.

[14] T. Lauritsen *et al*., Phys. Rev. Lett. **69**, 2479 (1992).

[15] M. Kaci *et al*., Z. Phys. A **354**, 267 (1996).

[16] K. Hauschild *et al*., Phys. Rev. C **55**, 2819 (1997).

[17] A. Lopez-Martens *et al*., Phys. Lett. **B380**, 18 (1996).

[18] A. Lopez-Martens *et al*., Phys. Rev. Lett. **77**, 1707 (1996).

[19] S. Siem *et al*., Phys. Rev. C **70**, 014303 (2004).

[20] T. L. Khoo *et al*., Phys. Rev. Lett. **76**, 1583 (1996).